Theoretical foundations for layered architectures and speed-accuracy tradeoffs in sensorimotor control

Yorie Nakahira[1], Quanying Liu[1], Natalie Bernat[1], Terry Sejnowski[2], John Doyle[1]

Abstract— Neuroscience provides rich details on sensorimotor control at both the system and component levels. Nervous systems sense, communicate, compute, and actuate movement, using distributed component hardware with tradeoffs in speed, accuracy, cost, sparsity, noise, and saturation throughout. The resulting control is nevertheless remarkably fast, accurate, robust, and efficient due to a highly effective layered architecture that combines higher layers of goals/plans/decisions/tracking with lower layer sensing/reflex/action. This paper addresses a gap in both neuroscience and control theory of a needed theoretical framework that clarifies and formalizes the connection between system and component level tradeoffs, how layered, distributed, and sparse control architectures are optimally organized, and why there is such extreme diversity within and across layers (from planning to reflex systems) and levels (brain systems to neural hardware components). We particularly emphasize speed-accuracy tradeoffs (SATs) which are ubiquitous in both neurophysiology and sensorimotor control. We characterize how the component SATs in spiking neuron communication and their sensory and muscle endpoints constrain the system SATs in both stochastic and deterministic models. Theoretically optimal layering creates "diversity sweet spots (DSSs), showing how to effectively layer sensorimotor control with appropriate diversity in neurons/muscles to achieve systems that are *both* fast and accurate despite being built from components that individually are not. Furthermore, the resulting optimal controllers for delayed/quantized systems and that of System Level Synthesis (SLS) for distributed/localized systems resemble the previously cryptic patterns of feedback and feedforward seen in vertebrate nervous systems, calling for further studies. A companion paper introduces simple demos and a new inexpensive and easy-to-use experimental platform that richly illustrate the theory and expand on the neuroscience motivation briefly reviewed here.

I. INTRODUCTION

To concretely illustrate speed-accuracy tradeoffs (SATs) in layered architectures consider riding a mountain bike down a twisting bumpy trail. There is an obvious tradeoff between speed down the trail, and accuracy in staying on it and not crashing. But exactly how is the system level that senses, communicates, computes, and actuates organized to allow experts to have extremely robust performance despite complex, uncertain environments and despite implementation in a hardware level of spiking neurons that is distributed, sparse, quantized, delayed, and/or saturating? A crucial strategy is the evolution of effective layered architectures that achieve remarkable robustness seamlessly integrate high-layer goals/plans/decisions that track the trail with low-layer sensing/reflex/action that handles bumps and is largely

[1]California Institute of Technology
[2]Salk Institute for Biological Studies and University of California San Diego
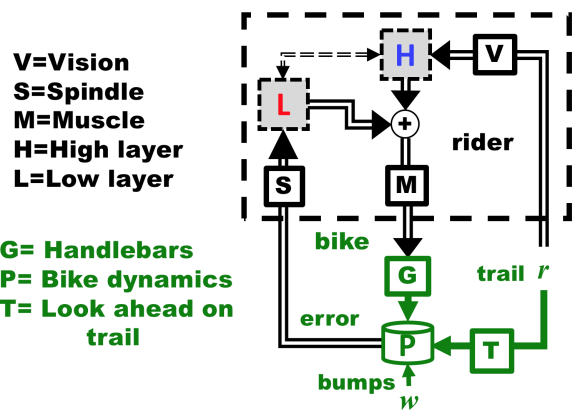
Fig. 1: Basic block diagram of a sensorimotor control model for a mountain bike and rider on a twisting trail with bumps. Each box is a component that communicates (V,S,M) or computes (H,L) using spiking neurons and thus has potentially both delay and quantization. The rider can see the trail ahead and thus has advanced warning T that would depend on speed and terrain, and can be used by the higher layer controller. The bumps are not seen but can crash the bike if not correctly handled by lower layer reflexes.

unconscious and automatic [1], [2].

Fig. 1 is a block diagram of a minimal and highly abstract model of the system level components involved in the biking problem, and also of the video game version presented in a companion paper (which includes a variety of additional illustrative demos). The plant **P** consists of bike and rider and is (possibly marginally) unstable, and must track a reference trail disturbance $r(t)$ with small error despite unseen bumps $w(t)$. Each box is designated by their function and either senses and communicates (vision **V**, muscle spindle sensor **S**) or actuates (muscle **M**) or computes a control action (high layer plan/track **H** and low layer reflex **L**). Each box can have quantization and/or delay and depending on the hardware level model details, stochastic noise and saturation. Vision gives the rider advance warning of the trail ahead, which is modeled here by a (variable) delay **T** between r and the plant that depends on speed, terrain, and the trail shape.

The theoretical challenge addressed here is to provide a framework that can compute optimally robust controllers for problems like Figure 1 with realistic models for r, w, and the components. We derive simple analytic formulas in important special cases that give striking insights, plus scalable algorithms for general problems. We also show that the key insights are remarkably robust to the assumptions (average vs. worst-case, stochastic vs. deterministic) provided they are
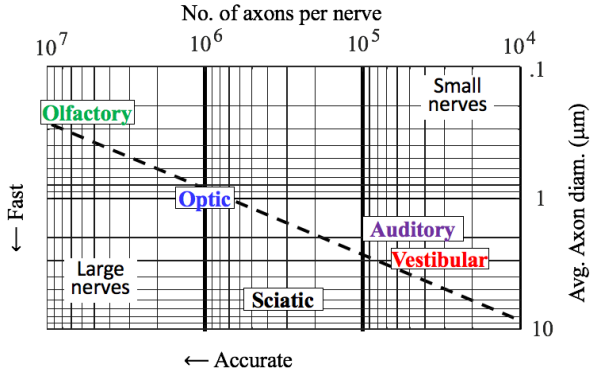
Fig. 2: Large diversity in the composition of selected human cranial and spinal nerves and the resulting speed-accuracy tradeoffs. The dashed line shows a constant total cross-sectional area, which is roughly proportional to the cost to build and maintain a nerve of a given length, and is similar across the different nerves, which are otherwise quite different. Our nerve model will translate axon size and number into biologically realistic delay and bandwidth, and the theory will then connect this hardware level SAT with system level SATs. This cartoon understates the diversity, both between the same nerve in different individuals, and between the axons within a single nerve, both of which are large and poorly characterized.

consistent at the system and component level. Perhaps most importantly we show how layering and sparse, distributed, localized control can create systems that are robust and biologically plausible by creating "diversity sweet spots" (DSSs). DSSs allow systems to be *both* fast *and* accurate despite being built from parts that are not.

DSSs appear everywhere in the nervous system and particularly in some of the components corresponding to Figure 1, as shown in the cartoon in Figure 2. Figure 2 shows selected cranial and spinal nerves (bundles of axons) including optic (vision) and vestibular and sciatic (reflexes). While they have similar total cross sectional areas (roughly proportional to the cost to build and maintain) they have extremely diverse compositions in terms of axon size and number [3–6]. As we will show, this translates directly into extreme tradeoffs in speed (in terms of delay) and accuracy (in terms of bandwidth), that then impose tradeoffs at the system level. Furthermore, optimal performance requires DSS in the layering of diverse controllers (Fig. 1), which are then built from diverse hardware components (e.g. Fig. 2).

While while modern lifestyles largely shield us from the challenges that shaped our brain's evolution, we see SAT and DSS appear everywhere in neuroscience, though the results are fragmented and incoherent, and even the terminology is not consistent. At the system level, the tradeoffs between speed and accuracy can be observed in diverse activities, from decisions [7] to reaching (Fitts' law) [8], [9] to sports (baseball, cricket, and soccer) [10], [11] (which perhaps more reflect our evolutionary past). An abundance of literature investigates the speed/accuracy tradeoffs in sensorimotor control from experimental data and

from conventional control theoretical perspectives, which do not account for hardware/communication constraints. Due to the lack of theoretical tools that integrate both levels and the resultant separate treatment of system and component levels, little attention has been paid to connecting the two levels, nor to clarifying the rich design tradeoffs and principles from a holistic perspective. This paper aims to fundamentally change this [12], [13].

Notation: We use $x(t_1 : t_2) = \{x(t_1), x(t_1 + 1), \cdots, x(t_2)\}$ to denote a truncated sequence. The ℓ_∞ norm of a sequence x is defined as $\|x\|_\infty := \sup_t |x(t)|$. We use $P(x)$ to denote the probability density function of a random variable x, and $P(x|y)$ to denote the conditional probability density function of x given another random variable y. We use $\log(x)$ to denote the logarithm of x in base 2 and $\log_b(x)$ to denote the logarithm of x in base b. We use $\mathbb{Z}/\mathbb{Z}_+$ and $\mathbb{R}/\mathbb{R}_+$ to denote the set of all/non-negative integers and the set of all/non-negative real numbers, respectively.

II. MAIN RESULTS

To clarify the fundamental limits of sensorimotor control imposed by hardware constraints, we present a mathematical framework of robust control involving sensing, communication, and actuation. This framework accommodates different assumptions on delay, data rate, and saturation in hardware and derive performance bounds in both deterministic worst case and stochastic average case.

In this section, we focus on a worst-case analysis, in contrast to the average-case. The worst-case and average-case analyses produce qualitatively similar results (Section IV-A). The worst-case, however, is more biologically plausible. In many sensorimotor tasks, there are strict error bounds which cannot be violated: for example, when riding a mountain bike on a cliff, not falling off the cliff is far more critical than minimizing average errors. The worst-case framework is also simpler than the average-case: deriving worst-case performance only requires high-school level mathematics, and thus has large potential in education and interdisciplinary research [13], [14].

Below, we summarize the SATs in spike-based neural signaling (Section II-A) and its impact on robust performance for systems whose performance bottleneck lies in the neural signaling (Section II-B–II-C). Closed-form performance bounds are derived for both a basic control system and a layered network with uniform/diverse nerves, and the resulting insights are consistent with those from alternative models/assumptions discussed in Section IV.

A. Component-level SATs

In a sensorimotor feedback loop, sensory information is transmitted by spikes (action potentials) through nerve fibers (axons). The space and metabolic constraints of a nerve limit the number and size of axons that can be built and maintained. These limits lead to SATs in neural signaling [3], [15], [16], and the specific forms of the SATs depend on how the nerves encode information (*e.g.* spike-based, spike-rate encoding). Below, we derive the SATs for spike-based

encoding in this section and discuss other alternatives in Section IV-B.

In a spike-based encoding scheme, information is encoded in the presence or absence of a spike in specific time intervals, analogous to digital packet-switching networks [17], [18]. This encoding method requires spikes to be generated with sufficient accuracy in timing, which has been experimentally verified in multiple types of neuron [19], [20]. To quantify the sometimes complex distributions of axon sizes in a single nerve, we can think of a nerve as being made up of several *communication channels*, each containing axons with identical size. We assume that there are m heterogeneous communication channels and index them by $i \in \{1, 2, \cdots, m\}$. We use n_i, ρ_i to denote the number of axons contained in channel i and the radius of axons in channel i, respectively. We use T_i, R_i to denote the delay and data rate (*i.e.* the amount of information in bits that can be transmitted) of channel i, respectively.

When the signaling is precise and noiseless, an axon with achievable firing rate ϕ can transmit

$$C_s = \phi \tag{1}$$

bits of information per unit time. For sufficiently large myelinated axons, the propagation speed $1/T_i$ and firing rate ϕ of action potentials are both approximately proportional to the axon radius ρ [3], *i.e.*

$$T = \alpha/\rho \qquad\qquad \phi = \beta\rho,$$

where α and β are proportionality constants. Moreover, the space and metabolic costs of a nerve are proportional to its volume [3], and given a fixed nerve length, these costs are proportional to its total cross-sectional area s. Using the above properties, we can show that[1]

$$R_i = \lambda_i T_i \qquad\qquad \sum_{i=1}^{m} \lambda_i = \frac{s\beta}{\pi\alpha} \tag{2}$$

A special case of (2) is when all axons are uniform, *i.e.* when ρ_i are identical for all i. In such a case, we can think of the nerve as a single communication channel with delay $T_s = T_i$ and $R = \sum_{i=1}^{m} R_i$ satisfying

$$R = \lambda T_s \qquad\qquad \lambda = \frac{s\beta}{\pi\alpha}. \tag{3}$$

B. System-level SATs

We consider a sensorimotor control model with the system dynamics

$$x(t+1) = ax(t) + w(t) + u(t) \tag{4}$$

where $x(t) \in \mathbb{R}$ is the state, $w(t) \in \mathbb{R}$ is the disturbance, $u(t) \in \mathbb{R}$ is the control action. We assume that the disturbance is ∞-norm bound and, without loss of generality, $\|w\|_\infty \leq 1$. The control action is generated through a feedback loop, which is constrained by data rate R, delay

T, and potentially saturation. The control action is generated by a controller K_t:

$$\begin{aligned} \mathcal{I}_t &= \{x(0:t), w(0:t+T_a), s(0:t-1)\} \\ [s_1(t), s_2(t), &\cdots, s_m(t)] = K_t(\mathcal{I}_t) \end{aligned} \tag{5}$$

and m quantizers:

$$u(t) = \sum_{i=1}^{m} Q_i(s_i(t - T_i - T_c)), \tag{6}$$

where Q_i has data rate R_i. So $R = \sum_{i=1}^{m} R_i$ is the number of bits per sampling interval that can be transmitted from the sensors to the actuators in the feedback loop. We additionally assume that the data rate is minimum stabilizing, *i.e.* $R > \log(|a|)$ [22]. The controller can access the disturbance information with an advanced warning of T_a, but its command is put into action with a delay of $T_i + T_c$, where T_i is the signaling delay satisfying the SAT (2) or (3), and $T_c \geq 0$ is other internal delays such as computation. We pose the robust control problem as follows:

$$\inf \sup_{\|w\|_\infty \leq 1} \|x\|_\infty, \tag{7}$$

where the infimum is taken over the control policies of the from (5) and (6). This robust control problem is motivated by sensorimotor tasks such as driving and riding a mountain bike (see Figure 1). In such tasks, $x(t)$ models the error between desired and actual trajectories; $u(t)$ models the control action taken by the sensorimotor system; and $w(t)$ models environmental noise and/or uncertainty in the desired trajectory (see our companion paper on experiments [14] for more detail).

The following lemma characterizes the performance limits on system robustness.[1]

Lemma 1: Let $\mathcal{R}: \mathbb{Z}_+ \to \mathbb{R}_+$ be defined to be

$$\mathcal{R}(h) := \sum_{i=1}^{m} \max\{0, h - T_i - T_c + T_a\} R_i.$$

The minimal state-deviation (7) is

$$\sum_{h=1}^{\infty} |a^{h-1}| \frac{1}{2^{\mathcal{R}(h)}}. \tag{8}$$

Formula (8) can be used to characterize the impact of instability. Specifically, the minimal state-deviation (7) of an unstable system with uniform axons (*i.e.* $|a| \geq 1$, $m = 1$) and $T_c - T_a = 0$ is given by[2]

$$\sup_{\|w\|_\infty \leq 1} \|x\|_\infty \geq \sum_{i=1}^{T} |a^{i-1}| + |a^T| \frac{1}{2^R - |a|}, \tag{9}$$

where the equality can be attained with minimal control effort

$$\sup_{\|w\|_\infty \leq 1} \|u\|_\infty = \left(|a^T| + \frac{|a^T|}{2^R - |a|}\right)\left(1 - \frac{1}{2^R}\right). \tag{10}$$

The control policy that achieves (9) and (10) is given in [12]. Interestingly, this optimal controller resembles predictive coding in neural signaling (see Section III-B for more detail).

Note that although unstable systems do not have a tradeoff between minimizing state-deviation and minimizing control effort, this property does not hold for stable systems, *i.e.* $|a| < 1$. In particular, the minimal state-deviation (7) of a stable system is given by[1]

$$
\begin{cases}
\displaystyle\sum_{i=1}^{T} |a^{i-1}| + |a^T| \frac{1}{2^R - |a|} & \text{if } \ell \le |a| \dfrac{2^R - 1}{2^R - |a|} \\
\displaystyle\sum_{i=1}^{T} |a^{i-1}| + |a^T| \frac{1-\ell}{1-|a|} & \text{otherwise.}
\end{cases}
$$

An important special case is the system with $a = 1$, which reduces to the setting of our driving game experiment and potentially other tasks such as riding a mountain bike [14] or eye movements [12], [13]. If such system is built from uniform axons, the minimal state-deviation (7) is given by

$$
\max(0, T_s + T_c - T_a) + \frac{1}{2^R - 1}. \tag{11}
$$

We can interpret the first term as the error due to delay, and the second term as the error due to quantization. Note that the impact of delay and quantization is experimentally verified in our driving game experiments [14].

If the system is built from two types of axons, *i.e.* $m = 2$, then (8) reduces to

$$
T_1 + \frac{1 - 2^{-R_1(T_2 - T_1)}}{2^{R_1} - 1} + \frac{1}{2^{R_1(T_2 - T_1)}} \frac{1}{2^{R_1 + R_2} - 1}. \tag{12}
$$

We can similarly interpret the first term as the error due to delay, and the second and third term as the error due to quantization. Combining (11) with (3) for uniform axons and (12) with (2) for diverse axons, we can obtain the system SATs in sensorimotor control.

C. SATs in a layered architecture

Previous sections describe the SATs at the component and system levels. In this section, we derive the SATs for layered architectures. Figure 1 sketches a minimal layered sensorimotor control model composed of higher-layer planning of trajectories and lower-layer reflex compensation to reject disturbance. The control commands from both layers are put into action by muscle. Specifically, we consider the system dynamics

$$
x(t+1) = ax(t) + u(t) + r(t) + w(t), \tag{13}
$$

where $r(t)$ models the changes in the desired trajectory, and $w(t)$ models the disturbance. We assume that $r(t), w(t)$ are ∞-norm bounded, and without loss of generality, $\|r\|_\infty \le 1$, $\|w\|_\infty \le \epsilon$. We consider two specific ways of layering: with and without sharing the disturbance information between the two controllers. The layered control system with shared

information is defined by

$$
\begin{aligned}
\mathcal{I}_t &= \{x(0:t), w(0:t), r(0:t+T_a)\} \\
u_h(t) &= H(\mathcal{I}_{t-T_h}, u(0:t-1)) \\
u_\ell(t) &= L(\mathcal{I}_{t-T_\ell-T_c}, u(0:t-1)) \\
u(t) &= Q_m(Q_\ell(u_\ell(0:t)), Q_h(u_h(0:t))).
\end{aligned} \tag{14}
$$

Here, H is a high-layer planner, L is a lower-layer disturbance compensator. The accuracy constraint of each controller is modeled by quantizers Q_ℓ/Q_h with data rates R_ℓ/R_h. The commands from both controllers are put into action by the muscle, whose accuracy is modelled by the quantizer Q_m with data rate R_m. The layering without shared information is defined by

$$
\begin{aligned}
u_h(t) &= H(r(0:t-T_h+T_a), u(0:t-1)) \\
u_\ell(t) &= L(w(0:t-T_\ell-T_c), u(0:t-1)) \\
u(t) &= Q_m(Q_\ell(u_\ell(0:t)), Q_h(u_h(0:t))).
\end{aligned} \tag{15}
$$

We pose the robust control problem as follows:

$$
\inf \sup_{\|w\|_\infty \le \epsilon, \|v\|_\infty \le 1} \|x\|_\infty, \tag{16}
$$

where the infimum is taken over the control policy with shared information (14) or that without shared information (15).

Let $\bar{R}_\ell$ and $\bar{R}_h$ are defined by

$$
\begin{aligned}
\bar{T}_\ell &:= T_\ell + T_c & \bar{R}_\ell &:= \min(R_\ell, R_m) \\
\bar{T}_h &:= T_h - T_a. & \bar{R}_h &:= \min(R_h, R_m)
\end{aligned}
$$

In the case with shared information, the minimum state-deviation (16) achievable by controller (14) is

$$
\left\{ \sum_{\tau=1}^{\bar{T}_\ell} |a^{i-1}| + \sum_{\tau=\bar{T}_\ell+1}^{\infty} \frac{|a^{i-1}|}{2^{\bar{R}_\ell(\tau-\bar{T}_\ell)+\bar{R}_h \max(0,\tau-\bar{T}_h)}} \right\} (1+\epsilon) \tag{17}
$$

The proof of (17) is an trivial extension of Lemma 1. When $a = 1$, (17) equals

$$
\left\{ \bar{T}_\ell + \frac{1 - 2^{-\bar{R}_\ell(\bar{T}_h - \bar{T}_\ell)}}{2^{\bar{R}_\ell} - 1} + \frac{1}{2^{\bar{R}_\ell(\bar{T}_h - \bar{T}_\ell)}} \frac{1}{2^{\bar{R}_\ell + \bar{R}_h} - 1} \right\} (1+\epsilon). \tag{18}
$$

In the case without shared information, the state-deviation (16) achievable by the controller (15) is lower-bounded by

$$
\left\{ \sum_{\tau=1}^{\bar{T}_\ell} |a^{i-1}| + \frac{|a^{\bar{T}_\ell}|}{2^{\bar{R}_\ell} - |a|} \right\} \epsilon + \sum_{\tau=1}^{\bar{T}_h} |a^{i-1}| + \frac{|a^{\bar{T}_h}|}{2^{\bar{R}_h} - |a|}. \tag{19}
$$

The performance limit (19) is a simple generalization of the results of [12, Section IV.C]. In the next section, we using these formulas to explore the benefit of axon diversity within/between levels and layers.

III. IMPLICATIONS

The results presented in Section II are first steps towards integrating the previously disjoint fields of neurophysiology and sensorimotor control, and towards providing a holistic perspective on high-layer planning and low-layer disturbance rejection. This perspective offers a more coherent view of the complex design space. In particular, it addresses how to exploit diversity both within a level and across layers to achieve fast and accurate system performance despite components that may be delayed or inaccurate.

Attaining optimal/robust performance requires two conditions: optimal components (hardware) and an optimal control/communication policy. To achieve the former condition, hardware needs to be built at a sweet spot in the component SAT in order to attain low delay and quantization costs at the system level. We show that such a sweet spot often lies at the position at which diverse nerves are used within a feedback loop, and at which diverse feedback loops are effectively layered (Section III-A). To achieve the latter condition, control/communication policy should have similar structures to optimal controllers in theory. Interestingly, the seemingly cryptic patterns of feedback and feedforward pathways seen in vertebrate nervous systems qualitatively resemble optimal controllers for delayed/quantized systems, as well as those from the System Level Synthesis (SLS) method [23] for distributed/localized systems (Section III-B).

A. Diversity sweet spots in SATs optimize performance

In sensorimotor control, it is well known that delays can cause small disturbances to end up as large errors [24]. Yet existing neurophysiology literature provides puzzling examples of sensorimotor nerves that are built toward achieving high data rates [25], despite the inherent delays incurred by such a property. Currently there exists no integrated theory that could rigorously explain how component SATs can be managed by neural systems to achieve good system performance. The results presented in Section II-B address this need, clarifying how to balance accuracy and speed subject to the component-level SATs.

Consider the special case of the worst-case state deviation for sensorimotor control in (11). Increasing signaling delay T_s incurs a corresponding linear penalty in the delay error T but leads to an exponential decrease in the quantization error. This property is experimentally verified in our driving game testbed [14]. Consequently, the minimum state-deviation is achieved at a sweet spot of intermediate levels of T_s and R.

The exact position of the sweet spot depends on $T_c - T_a$. For systems with a large delay (i.e. positive $T_c - T_a$), the cost due to delay dominates the total cost, so minimizing T_s at the expense of small R leads to optimal performance. For systems with a large advance warning (i.e. negative $T_a - T_c$), the cost due to quantization dominates the total cost, so maximizing data rate R at the expense of large T_s leads to better performance.

The framework developed in section II-B can further describe the effects of diversity in neural composition on
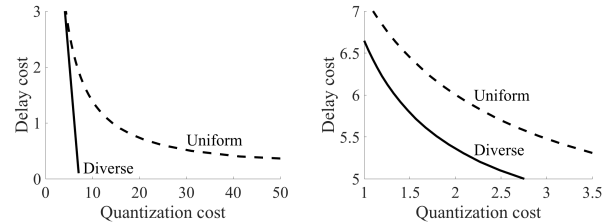
Fig. 3: The benefit of within-level (left) and layering (right) diversity. We use $m = 1$ for uniform nerves and $m = 2$ for diverse nerves, and we set $s\beta/(\pi\alpha) = 1$ and $T_i - T_a = 0$. In both cases, introducing diversity enables the system to achieve better SAT performance.

performance. For the system with uniform nerves, we associate its speed/accuracy with the delay/quantization costs in (11). For systems with diverse communication channels, we find its speed to be T_1 in (12), i.e. the errors before the first packet arrives, and its accuracy to be the remaining terms in (12). In Figure 3 (right), we see that systems with diverse nerves have an improved SAT compared with systems with uniform nerves. These results suggest that a system made of nerves that are not uniformly fast and accurate, but rather are diverse in composition, can achieve performance as though they were indeed uniformly fast and accurate. We name this kind of effective architecture a *diversity sweet spot* (DSS).

Similarly, the results of section II-C demonstrate another DSS and the benefit of diversity between layers. Figure 4 (left) compares the performance lower-bounds (19) for the layered system without shared information (13), (15) when the delay and data rate of the higher-layer (T_ℓ, R_ℓ) and those of the lower-layer (T_h, R_h) are allowed to be diverse or are constrained to be uniform.[3] The performance gain is especially high when the two layers are heterogeneous, i.e. large $T_c - T_a$ (Figure 4), demonstrating the benefit of using diverse nerves between high and low layers. A similar DSS can be observed in an alternative setting of shared information, whose performance lower-bound is given by (18). The results suggest that layered architectures of diverse control loops, if well-exploited, help achieve fast and accurate sensorimotor performance despite the speed and accuracy constraints of individual layers.

Delving further into this example, we observe DSSs in the hardware that achieves this optimal system performance. The optimal nerves for (19) with $m = 2$ have consistently small T_ℓ to control the cost of delay, but allows R_h to increase for large advanced warning T_a (Figure 4, right).

It is important to note that the properties we have found to be optimal are indeed observed in nature. As seen in Figure 2, the communication channels involved in our many sensory modalities span the range of the SAT. Further, the distributions of axons within nerves are highly diverse, especially those involved in sensorimotor control like the optic, vestibular, and sciatic nerves. These observations indicate that a diversely layered control architecture composed of

---

[3]Here, we assume that R_m is sufficiently large.
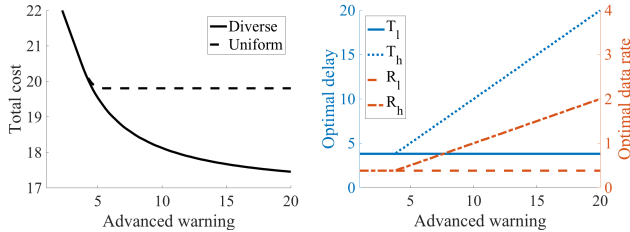
Fig. 4: The benefit of nerve diversity in layered architectures. The left shows the minimum state-deviation (19) for varying advanced warning T_a in the case when *diverse* delays and data rates of L and H are allowed, versus the case when only *uniform* delays and data rates are permitted (*i.e.* $R_\ell = R_h$ and $T_\ell = T_h$). Other parameters are set to be $R_\ell = 0.1T_s$, $R_h = 0.1T_h$, and $T_c = 10$. The right shows the resulting optimal delays and data rates for the diverse case.

diversely distributed axon sizes is plausible within the limits of observed neurophysiology.

B. Optimal controller structures resemble predictive coding

Predictive coding is a ubiquitous process throughout the human brain, appearing across sensing, cognition, and control systems [26]. It is a compressed representation strategy, wherein a system maintains an internal model of an incoming signal; the model is used to predict future content of the signal, the incoming signal is compared to the prediction, and only the so-called prediction error needs to be communicated back to the internal model in order to convey the information in the incoming signal. Although a complex internal model must be built and maintained, this strategy drastically reduces the information that must be communicated in feedback loops.

Interestingly, structures resembling predictive coding emerge naturally in optimal controllers for delayed/quantized systems (Section II-B) and that of System Level Synthesis (SLS) for distributed/localized systems [23]. For a scalar system (4), the optimal controller for (7) is given by:

$$K : u^*(t) = -A^T w(t - T) - A(u(t-1) - u^*(t-1))$$

and a uniform quantizer Q_R in the interval $[-L, L]$, where $L = |a^T| + |a^{T+1}|/(2^R - |a|)$. On the other hand, the optimal controller given by the System Level Synthesis (SLS) methods has a procedure to estimate $w(t)$ and $x(t)$ (involving $\hat{w}(t)$ and $\hat{x}(t)$ in [23]), which are then used to compute the control actions. In both cases, the system first obtains the disturbance information and uses it to predict future states; the state prediction is then compared with the actual value, and only the error signal needs to be sent through nerves.

IV. ALTERNATIVE MODELS

The framework presented in Section II allows us to accommodate different assumptions and models. In this section, we study a few alternative assumptions: the average-case analysis of a stochastic sensorimotor control setting (Section IV-A), different types of neural encoding (Section IV-B), and muscle actuation including reaching tasks (Section IV-C).

A. Average case analysis of a stochastic system

Section II provides a worst-case analysis of a deterministic system with bounded noise and quantizers. Here, we consider the average case when the disturbance is stochastic and the mutual information between the sensor measurements and control actions are limited by the constraints of the neural signaling capability.

We consider a uniform feedback control model with the system dynamics (4), where $\{w(t)\}$ is a sequence of *i.i.d.* random variables with mean 0 and variance 1. The controller K is composed of an encoder and a decoder. At time t, the encoder uses $x(0, t)$, $w(0, t)$, and $s(0 : t)$ to generate a channel input $s^*(t)$ according to the probability density function $P(s^*(t)|x(0, t), w(0, t), s(0 : t - 1))$. Then, a communication channel sends $s^*(t)$ to the decoder with delay $T \geq 0$, so $s^*(t)$ is received at time $t + T$ as $s(t)$ with potential error/noise. Then, the decoder generates a control action $u(t+T)$ according to the probability density function $P(u(t + T)|s(0 : t))$. The communication channel also constraints the amount of information the feedback loop can transmit, and this constraint is written as

$$\lim_{n \to \infty} \frac{1}{n} I(x(0 : n - T); u(0 : n)) \leq R. \tag{20}$$

We consider minimizing the following mean-squared state deviation:

$$\inf \lim_{n \to \infty} \frac{1}{n} \sum_{t=1}^{n} \mathbb{E}[x(t)^2] \tag{21}$$

where the infimum is taken over all control and communication policy of the form $P(u(t)|x(0 : t - T), u(0 : t - 1))$ satisfying the communication constraints (20) and saturation constraints

$$\lim_{n \to \infty} \frac{1}{n} \sum_{t=1}^{n} \mathbb{E}[u(t)^2] \leq \ell. $$

We assume that the data rate is minimum stabilizing, *i.e.* $R > \log(|a|)$ [22]. We adapt the results of control under information constraints [27–30] to explicitly characterize the impact of information constraints, delay, and saturation.

Let $P : \mathbb{R}_+ \to \mathbb{R}_+$ and $G : \mathbb{R}_+ \to \mathbb{R}_+$ be functions given by

$$P(\lambda) = \frac{1}{2} \left\{ 1 - \lambda + a^2\lambda + \sqrt{4\lambda + (a^2\lambda - \lambda + 1)^2} \right\}$$

$$G(\lambda) = \frac{a^2 P^3 (a^2\Lambda + a^{2(T+1)} - \Lambda)}{P^2 + 2\lambda P + \lambda^2 + \lambda a^2 P^2},$$

where $\Lambda = a^{2(T+1)}/(2^{2R} - a^2)$. When $\ell < G(0)$, we define λ^* to be the strictly positive scalar that satisfies[4]

$$G(\lambda^*) = \ell. \tag{22}$$

---

[4]Observe that $G(\lambda) \geq 0$ by construction. In addition, the solution of (22) is unique.

When $\ell \geq G(0)$, we set $\lambda^* = 0$. Given such λ^*, we define the scalars P^* and G^* to be $P^* = P(\lambda^*)$ and $G^* = G(\lambda^*)$, respectively. The fundamental limits in performance is given below.[1]

Lemma 2: The minimal state-deviation (21) is[2]

$$\left\{\sum_{i=1}^{T} a^{2(i-1)}\right\} + P^* a^{2(T+1)} + \frac{a^{2(T+1)}(P^* a^2 - P^* + 1)}{2^{2R} - a^2},$$

which can be achieved with the control effort $\lim_{n\to\infty}(1/n)\sum_{t=1}^{n}\mathbb{E}[u(t)^2] = G(\lambda^*)$.

A special case of Lemma 2 is when $a = 1$ and $\ell = \infty$. In this case, we have $\lambda^* = 0$, $P(\lambda^*) = 1$, $G(\lambda^*) = 1$, and thereby

$$\inf \lim_{T\to\infty} \frac{1}{T}\sum_{t=1}^{T}\mathbb{E}[x(t)^2] = T + \frac{1}{2^{2R}-1}$$

Interestingly, though the control effort generally depends on the data rate, at $a = 1$, $\lim_{n\to\infty}(1/n)\sum_{t=1}^{n}\mathbb{E}[u(t)^2] = 1$ does not.

B. Sensory nerve signaling

The information in spikes can hypothetically be encoded in many different ways [17], [19], [20], [31]. While section II-A characterizes the neural signaling SATs assuming that a nerve encode information in individual spikes, this section derives the SATs under an alternative assumption: that a nerve encode information in spike rates [32]. We can think of the rate-based encoding as a Poisson-type communication channel whose input is the spike rate $\gamma(t)$ and the output is the spike timing $M(t)$. We assume that the spike timing is a non-homogeneous Poisson point process with rate (intensity) $\gamma = \{\gamma(t) \geq 0 : t \in \mathbb{R}_+\}$, denoted by $\mathcal{P}_t(\gamma)$. The communication channel is then given by

$$M(t) = \mathcal{P}_t(\gamma).$$

where the spike rate is bounded by

$$\gamma(t) \leq \phi \qquad\qquad t \in \mathbb{R}_+, \qquad (23)$$

for some $\phi > 0$. The information capacity of communication channel (23) is defined to be

$$C_r = \sup \lim_{T\to\infty} \frac{1}{T} I(\gamma^T; M^T),$$

where the supremum is taken over all distributions of the input process $\mathcal{P}_{\gamma(t)}$ satisfying (23). Kabanov has shown in [33] that C_r is upper-bounded by

$$C_r = \frac{(\phi+1)^{1+\phi^{-1}}}{2} - \left(1 + \frac{1}{\phi}\right)\log(\phi+1) \qquad (24)$$

So for sufficiently large ϕ,

$$C_r \to \phi/2 \quad \text{as } \phi \to \infty. \qquad (25)$$

Similarly to Section II-A, we obtain

$$R_i = \lambda_i T_i \qquad\qquad \sum_{i=1}^{m}\lambda_i = \frac{s\beta}{2\pi\alpha}. \qquad (26)$$

	Bits per time	SATs
Spike-based	ϕ	$s\beta T = 2\pi\alpha R$
Rate-based	$\phi/2$	$s\beta T = \pi\alpha R$

TABLE I: Efficiency of different neural signaling schemes

The SATs (2) and (26) suggest that spike-based encoding allows more information to be transmitted than rate-based encoding under the same maximum spike rate ϕ, Interestingly, the SATs of spike-based encoding and rate-based encoding have qualitatively similar SATs: given a fixed resource (space and metabolic cost to build and maintain a never), the achievable data rate is roughly proportional to delay.
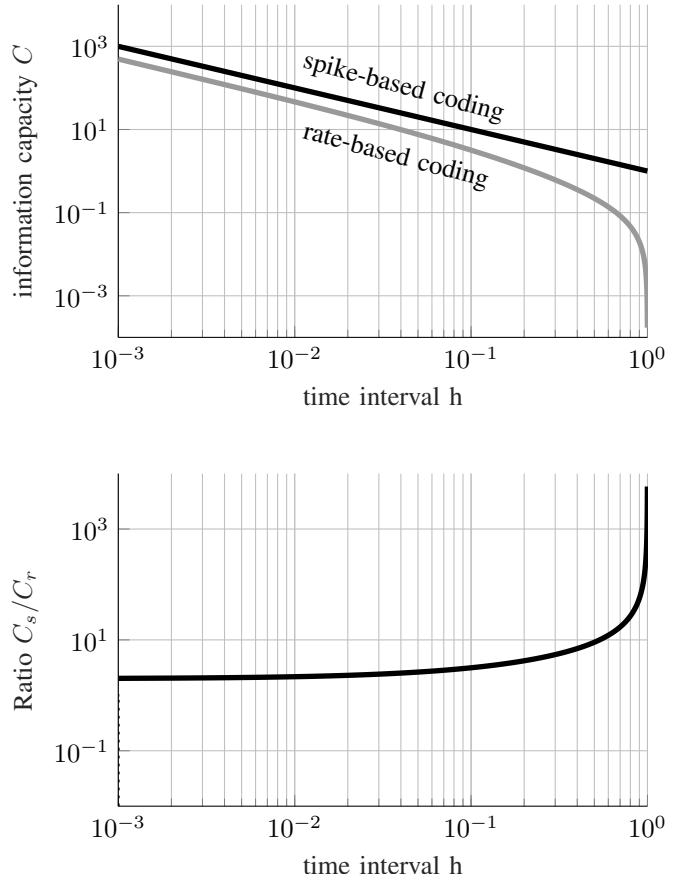
Fig. 5: Information capacity of spike-based coding (1) and that of rate-based encoding (25) for a fixed achievable time interval h.

C. SAT in muscle actuation and reaching tasks

In this section, we present another component and system SATs that illustrate the DDS, involving muscle actuation and reaching tasks. We consider a simplified muscle model which includes m motor units, indexed by $i \in \{1, 2, \cdots, m\}$, each associated with a reaction speed and a strength level. We use F_i to denote its strength and assume without loss of generality that $F_1 \leq F_2 \cdots \leq F_m$. Motor units are recruited in ascending order of F_i, so a muscle (at non-transient time)

can only generate $m+1$ levels of discrete strength levels: $\sum_{i=1}^{n} F_i$, $n \in \{0, 1, 2, \cdots, m\}$.[1] Because the strength of a motor unit is roughly proportional to its cross-sectional area (myofibril cross-sectional area) [34], given a fixed lengths, the maximum strength of a muscle $\ell = \sum_{i=1}^{m} F_i$ is proportional to its cross-sectional area. This implies that, given a fixed space to build a muscle, its maximum strength does not depend on the specific composition of motor units.

Given a fixed maximum strength ℓ, there is a tradeoff between a muscle's reaction speed and resolution. Specifically, if a motor unit is recruited at time $t = 0$, then its strength $c_i(t)$ raises according to[1]

$$\dot{a}_i(t) = \alpha f_i^p(1 - a_i(t)) - \beta a_i(t) \quad a_i^q(t) = c_i(t) \quad (27)$$

with the initial condition $c_i(0) = 0$ and $f_i = 1/((\gamma/F_i)^{1/q} - 1)$ [5].[5] Similarly, when a recruited motor unit is released at time $t = 0$ its contraction rate falls according to (27) with $f_i = 0$ and $c_i(0) = F_i$. The relation (27) indicates that the reaction speed of a muscle is an increasing function of F_i.[6] Constrained by $\ell = \sum_{i=1}^{m} F_i$, a muscle can be built from many motor units with small strengths or a few motor units with large strengths. In the former case, the muscle has better resolution but slow reaction speed, while in the latter case, the muscle has fast reaction speed but coarser resolution.
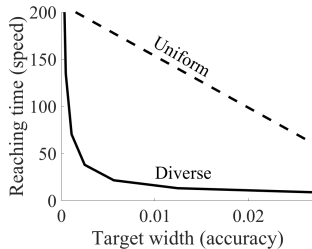
Fig. 6: The SAT in a reaching task imposed by the SAT of a muscle with uniform versus diverse motor units. For a fixed sensorimotor control sampling interval, an upper bound $\bar{F}$ on the strength of recruitable motor units is obtained from the target width (accuracy requirement) using (27). Then, from $\bar{F}$, the reaching time is computed using (27) for the case of recruiting all motor units with strength below $\bar{F}$.

This component SAT leads to a system SAT in a reaching task. Consider reaching a hand towards a target of width D located at a fixed distance (a task typically associated with Fitts Law). In this task, the reaching time provides a measure of speed and the target width is a measure of accuracy. Figure 6 shows this maximum reaching time (speed) given a fixed target width (accuracy). When we naively build a muscle using uniform motor units, the SAT has a linear form, which is inconsistent with standard experiments. However, *diversity* in motor units achieves a logarithmic SAT, yielding a DSS in which both speed and accuracy can be achieved. Although

this logarithmic SAT has been observed in the context of Fitts law, the connection between the logarithmic nature of Fitts law and the notion of DSS has not previously been made.

V. Conclusion

We have presented the foundations of a control theoretic framework that integrates previously disparate subfields of surrounding sensorimotor control. This framework clarifies the relationships between component properties, architectural organization, and system performance in the context of SATs. The framework is flexible enough to accommodate a variety basic assumptions about the underlying systems that it represents and its results are consistent with natural observations from sensorimotor control and neurophysiology.

References

[1] N. Lan, V. C. Cheung, and S. C. Gandevia, "Neural and computational modeling of movement control," *Frontiers in computational neuroscience*, vol. 10, p. 90, 2016.

[2] J. C. Doyle and M. Csete, "Architecture, constraints, and behavior," *Proceedings of the National Academy of Sciences*, vol. 108, no. Supplement 3, pp. 15 624–15 630, 2011.

[3] P. Sterling and S. Laughlin, *Principles of neural design*. MIT Press, 2015.

[4] C. J. De Luca and Z. Erim, "Common drive of motor units in regulation of muscle force," *Trends in neurosciences*, vol. 17, no. 7, pp. 299–305, 1994.

[5] V. Brezina, I. V. Orekhova, and K. R. Weiss, "The neuromuscular transform: the dynamic, nonlinear link between motor neuron firing patterns and muscle contraction in rhythmic behaviors," *Journal of neurophysiology*, vol. 83, no. 1, pp. 207–231, 2000.

[6] S. Li, C. Zhuang, M. Hao, X. He, J. C. Marquez Ruiz, C. M. Niu, and N. Lan, "Coordinated alpha and gamma control of muscles and spindles in movement and posture," *Frontiers in computational neuroscience*, vol. 9, p. 122, 2015.

[7] R. P. Heitz, "The speed-accuracy tradeoff: history, physiology, methodology, and behavior," *Frontiers in neuroscience*, vol. 8, p. 150, 2014.

[8] P. M. Fitts and J. R. Peterson, "Information capacity of discrete motor responses." *Journal of experimental psychology*, vol. 67, no. 2, p. 103, 1964.

[9] R. W. Soukoreff and I. S. MacKenzie, "Towards a standard for pointing device evaluation, perspectives on 27 years of fitts law research in hci," *International journal of human-computer studies*, vol. 61, no. 6, pp. 751–789, 2004.

[10] J. Freeston and K. Rooney, "Throwing speed and accuracy in baseball and cricket players," *Perceptual and motor skills*, vol. 118, no. 3, pp. 637–650, 2014.

[11] R. van den Tillaar and A. Ulvik, "Influence of instruction on velocity and accuracy in soccer kicking of experienced soccer players," *Journal of motor behavior*, vol. 46, no. 5, pp. 287–291, 2014.

[12] Y. Nakahira, N. Matni, and J. C. Doyle, "Hard limits on robust control over delayed and quantized communication channels with applications to sensorimotor control," in *Decision and Control (CDC), 2015 IEEE 54th Annual Conference on*. IEEE, 2015, pp. 7522–7529.

[13] J. Doyle, Y. Nakahira, Y. P. Leong, E. Jenson, A. Dai, D. Ho, and N. Matni, "Teaching control theory in high school," in *Decision and Control (CDC), 2016 IEEE 55th Conference on*. IEEE, 2016, pp. 5925–5949.

[14] Q. Liu, Y. Nakahira, A. Mohideen, S. Choi, and J. C. Doyle, "A experimental platform to study the speed/accuracy tradeoffs and layered architectures in human sensorimotor control," submitted to ACC2019.

[15] J. A. Perge, K. Koch, R. Miller, P. Sterling, and V. Balasubramanian, "How the optic nerve allocates space, energy capacity, and information," *Journal of Neuroscience*, vol. 29, no. 24, pp. 7917–7928, 2009.

[16] J. A. Perge, J. E. Niven, E. Mugnaini, V. Balasubramanian, and P. Sterling, "Why do axons differ in caliber?" *Journal of Neuroscience*, vol. 32, no. 2, pp. 626–638, 2012.

[17] E. Salinas and T. J. Sejnowski, "Correlated neuronal activity and the flow of neural information," *Nature reviews neuroscience*, vol. 2, no. 8, p. 539, 2001.

---

[5] Here, $\alpha = 1, \beta = 1, p = 1$ are fixed constants, chosen to be standard values suggested in [5].

[6] In other words, the time required for a muscle to reach to $c_i(t) = F_i$ from $c_i(0) = 0$ is decreasing in F_i.

[18] K. H. Srivastava, C. M. Holmes, M. Vellema, A. R. Pack, C. P. Elemans, I. Nemenman, and S. J. Sober, "Motor control by precisely timed spike patterns," *Proceedings of the National Academy of Sciences*, vol. 114, no. 5, pp. 1171–1176, 2017.

[19] Z. F. Mainen and T. J. Sejnowski, "Reliability of spike timing in neocortical neurons," *Science*, vol. 268, no. 5216, pp. 1503–1506, 1995.

[20] J. L. Fox, A. L. Fairhall, and T. L. Daniel, "Encoding properties of haltere neurons enable motion feature detection in a biological gyroscope," *Proceedings of the National Academy of Sciences*, p. 200912548, 2010.

[21] Y. Nakahira, Q. Liu, N. Bernat, T. Sejnowski, and J. C. Doyle. Theoretical foundations for layered architectures and speed-accuracy tradeoffs in sensorimotor control. [Online]. Available: http://users.cms.caltech.edu/~ynakahir/

[22] G. N. Nair, F. Fagnani, S. Zampieri, and R. J. Evans, "Feedback control under data rate constraints: An overview," *Proceedings of the IEEE*, vol. 95, no. 1, pp. 108–137, 2007.

[23] Y.-S. Wang, N. Matni, and J. C. Doyle, "A system level approach to controller synthesis," *arXiv preprint arXiv:1610.04815*, 2016.

[24] Y. P. Leong and J. C. Doyle, "Understanding robust control theory via stick balancing," in *Decision and Control (CDC), 2016 IEEE 55th Conference on*. IEEE, 2016, pp. 1508–1514.

[25] W. Bialek, F. Rieke, R. van Steveninck, and D. Warland, "Spikes: Exploring the neural code," 1999.

[26] P. K. H. Ouden and F. Lange, "How prediction errors shape perception, attention, and motivation," *Frontiers is Psychology*, 2012.

[27] S. Tatikonda, A. Sahai, and S. Mitter, "Stochastic linear control over a communication channel," *IEEE transactions on Automatic Control*, vol. 49, no. 9, pp. 1549–1561, 2004.

[28] T. Tanaka, P. M. Esfahani, and S. K. Mitter, "Lqg control with minimum directed information: Semidefinite programming approach," *IEEE Transactions on Automatic Control*, vol. 63, no. 1, pp. 37–52, 2018.

[29] V. Kostina and B. Hassibi, "Rate-cost tradeoffs in control," in *Communication, Control, and Computing (Allerton), 2016 54th Annual Allerton Conference on*. IEEE, 2016, pp. 1157–1164.

[30] Y. Nakahira, F. Xiao, V. Kostina, and J. C. Doyle, "Fundamental limits and achievable performance in biomolecular control," in *2018 Annual American Control Conference (ACC)*. IEEE, 2018, pp. 2707–2714.

[31] C. Bodelon, M. Fallah, and J. H. Reynolds, "Temporal resolution of the human visual system for processing color, orientation, and color/orientation conjunctions," *Journal of Vision*, vol. 5, no. 8, pp. 758–758, 2005.

[32] R. G. R. Stein and K. Jones, "Neuronal variability: noise or part of the signal?" *Nature Reviews Neuroscience*, 2005.

[33] H. A. M. Davis, "Capacity and cutoff rate for poisson-type channels," *IEEE Transactions on Information Theory*, vol. 26, no. 6, pp. 710–715, 1980.

[34] G. Goldspink, "Malleability of the motor system: a comparative approach," *Journal of experimental biology*, vol. 115, no. 1, pp. 375–391, 1985.